Oxidation Catalysis by Oxide-Supported Au Nanostructures: The Role of Supports and the Effect of External Conditions

Siris Laursen and Suljo Linic*

Department of Chemical Engineering, University of Michigan, Ann Arbor, Michigan 48109-2136, USA

(Received 25 April 2006; published 14 July 2006)

Oxide-supported Au nanostructures are promising low-temperature oxidation catalysts. It is generally observed that Au supported on reducible oxides is more active than Au supported on irreducible oxides. Recent studies also suggest that cationic $Au^{\delta+}$ is responsible for the unique Au/oxide catalytic activity, contrary to the conventional perception that oxide supports donate electronic charge to Au. We have utilized density functional calculations and *ab initio* thermodynamic studies to investigate the oxidation state of Au nanostructures deposited on reducible and irreducible supports. We find that there are fundamental differences in the electronic structure of Au deposited on the different oxides. We propose a simple model, grounded in the first principles calculations, which can explain the oxide-specific catalytic activity of Au nanostructures and which can account for the presence and the role of cationic $Au^{\delta+}$.

DOI: 10.1103/PhysRevLett.97.026101 PACS numbers: 82.65.+r, 68.43.Bc, 68.43.De, 82.20.Db

Gold (Au) is chemically inert. However, Au nanoparticles and nanofilms deposited on oxide supports are active in a number of catalytic reactions including low-temperature CO oxidation and propylene epoxidation [1,2]. Even though oxidation reactions over Au/oxide catalysts have been studied extensively, there are many fundamental questions that remain unanswered. There is an intensive debate regarding the oxidation state of catalytically active Au [3–8]. While ultrahigh vacuum (UHV) studies and theoretical calculations suggest that electronic charge is transferred from a support to Au yielding anionic $Au^{\delta-}$ [3,6,8], steady-state experiments suggest that cationic (oxidized) $Au^{\delta+}$ is responsible for the unusual activity [4,5]. Another question that has been argued extensively is whether and how oxide supports impact the catalytic activity. It has been demonstrated that Au supported on reducible oxides (TiO_2, Fe_2O_3) is more active than Au supported on irreducible oxides (SiO_2, Al_2O_3) under similar conditions and for Au particles of identical size [9,10]. Irreducible oxides are characterized by higher metal-oxygen bond strength and larger band gap than reducible oxides.

In this Letter, density functional theory (DFT) and *ab initio* thermodynamic calculations have been utilized to investigate (i) the oxidation state of catalytically active Au and (ii) the role of oxide supports. We focus on pressure- and temperature-dependant interactions of oxygen with Au deposited on a reducible (TiO_2) and an irreducible (SiO_2) oxide. We demonstrate that the oxidation state of Au is governed by external conditions (oxygen pressure and temperature) and by the chemical interactions between oxides and Au. We find that while under low oxygen chemical potentials, electron density is transferred from an oxide support to Au forming $Au^{\delta-}$; under catalytically relevant conditions there exists a thermodynamic driving force to oxidize $Au^{\delta-}$ and form cationic $Au^{\delta+}$. Our calculations show that highly anionic $Au^{\delta-}$, formed when Au is deposited on reducible TiO_2, interacts strongly with oxygen and is easily oxidized even at moderate oxygen chemical potentials. On the other hand, mildly anionic $Au^{\delta-}$, formed when Au is adsorbed on irreducible SiO_2, interacts weakly with oxygen and high oxygen chemical potentials are required to oxidize the substrate. We propose a simple model, grounded in the first principles calculations, which can explain the oxide-specific catalytic activity of Au nanostructures adsorbed on oxide supports.

We utilize a model system with an Au(111) bilayer adsorbed epitaxially on an oxygen-vacancy-rich (4×1) unit cell of rutile $TiO_2(110)$ and $SiO_2(110)$, see Fig. 1. Rutile is thermodynamically the most stable phase of TiO_2, while rutile SiO_2 is metastable under relevant conditions. We explore the oxide supports with oxygen vacancies, labeled R-TiO_2 and R-SiO_2, since it has been observed that the vacancy sites serve as anchoring points for Au nanoclusters [11]. These model systems, which are struc-

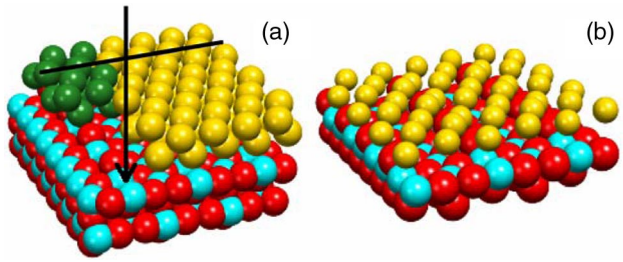

FIG. 1 (color online). (a) The model system contains an Au(111) bilayer adsorbed on rutile $TiO_2(110)$-(4×1) and $SiO_2(110)$-(4×1). The unit cell is colored in green. The arrow points towards an oxygen vacancy. The dark line depicts the direction of the Au stretch required to accommodate the TiO_2 lattice. There is no stretch for Au supported on SiO_2. O atoms are red, Ti or Si are blue, while Au is yellow. (b) The layer of Au, bonded to the support, is depicted. Notice the relaxation of Au atoms towards oxide vacancies.

turally almost identical for both oxides, allow us to focus on the support-specific aspects of Au/oxide chemistry. A similar model system containing an Au bilayer adsorbed on TiO_2 has been found to exhibit superior CO-oxidation activity in well-controlled high vacuum experiments [12]. The oxide surface is modeled with 50% of the bridge oxygen atoms missing. The Au bilayer is oriented so that the Au lattice stretch, caused by the lattice mismatch between Au and the oxides, is minimized for the explored (4×1) oxide unit cell. This orientation yields the TiO_2-induced Au lattice stretch of $\sim$12% in the [112] direction, consistent with the experimentally reported values [13], and no stretch or compression for Au on SiO_2. The lattice constants of the Au/oxide systems have also been optimized in the DFT calculations which showed that the lowest energy state is the one where the bilayer accommodates the lattice constant of the underlying oxide support.

Oxygen adsorption is modeled by oxygen atoms occupying threefold hollow sites on the Au surface and interstitial Au subsurface sites [5]. Figure 2 shows the surface free energy of adsorption [14] calculated for oxygen adsorbed on Au(111), Au supported on R-TiO_2, and Au supported on R-SiO_2 as a function of oxygen chemical potential [15,16]:

$$\Delta G(T,P) = \frac{N}{A}[E_{\text{ads}} - \Delta\mu_O(T,P)] = \frac{N}{A}\left[E_{\text{ads}} - \mu_O(T,P^o) - \frac{1}{2}kT\ln\left(\frac{P}{P^o}\right)\right].$$

N is the number of oxygen atoms per unit cell while A is the surface area of the unit cell. The adsorption energy (E_{ads}) per $\frac{1}{2}$ O_2 is obtained as $E_{\text{ads}} = 1/N[E$ (oxidized substrate)-E(substrate)$-N/2E(O_2)]$, where the relevant energies are calculated in the DFT calculations. Temperature and pressure effects on the free energy of O_2 are included through $\Delta\mu_O$ which can be computed from first principles using appropriate partition functions or obtained from thermochemical tables [17]. We note that metal-oxygen vibrations, which are approximated to contribute a maximum of ± 2.3 meV/Å^2 at 300 K, and slab phonon contributions, which to a large extent cancel each other in the formulation of the free energy, are neglected.

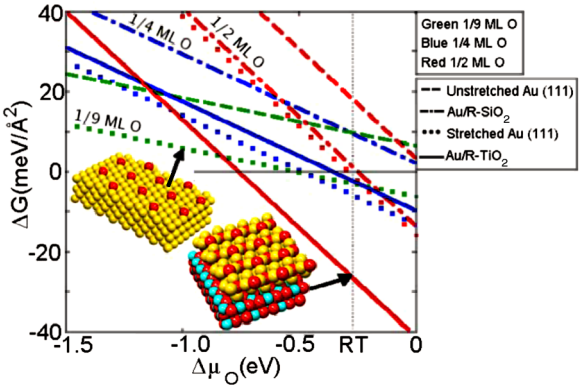

FIG. 2 (color online). Surface Gibbs free energy of adsorption for oxygen adsorbed on Au(111), stretched Au(111), Au/R-TiO_2 and Au/R-SiO_2. The horizontal line zero corresponds to clean (no oxygen adsorption) substrate. The vertical $\Delta\mu_O = 0$ line corresponds to the energy of $\frac{1}{2}$ O_2 at $T = 0$ K and standard pressure. Insets show the most stable configurations for $\frac{1}{9}$ ML oxygen adsorbed on stretched Au(111) and $\frac{1}{2}$ ML adsorbed on the Au/R-oxide system.

The configuration with the lowest free energy at a given oxygen chemical potential is thermodynamically the most stable at the external conditions (pressure and temperature) that correspond to the chemical potential. The term "the most stable structure" refers to the energetically favorable structure among the tested trial structures. While one cannot exclude the possible existence of other more stable configurations, this uncertainty has little effect on our conclusions. Figure 2 shows that oxygen adsorption on Au (111) (dashed lines) is thermodynamically unfavorable for all realistic oxygen chemical potentials. This observation corroborates the chemical inertness of Au. Figure 2 also shows that oxygen does not adsorb on Au/R-SiO_2 (dash-dotted lines) at the chemical potentials lower than ~ -0.27 eV [this corresponds to atmospheric pressure and room temperature (RT)]. However, at the chemical potentials higher than -0.27 eV, the most stable configuration has $\frac{1}{2}$ ML of oxygen adsorbed. In this configuration, which is effectively a 2D surface oxide, $\frac{1}{4}$ ML oxygen is adsorbed on the Au surface and $\frac{1}{4}$ ML is in the Au subsurface sites close to the oxygen vacancy. In the case of Au/R-TiO_2 (full lines), the $\frac{1}{2}$ ML oxidic structure is thermodynamically the most stable even at very low oxygen chemical potentials ($\Delta\mu_O > -0.7$ eV).

Since Au adsorbed on R-TiO_2 is slightly stretched, it is important to decouple the stretching effect from the electronic effect due to the chemical interactions between Au and R-TiO_2. To decouple these effects we have studied oxygen adsorption on stretched but unsupported Au(111) (dotted lines). The Au(111) lattice is stretched so that the lattice constant corresponding to Au/R-TiO_2 is reproduced. Figure 2 shows that while on Au/R-$TiO_2$the $\frac{1}{2}$ ML oxidic structure is the most stable for a wide range of external conditions, on stretched Au(111) the most stable configuration has oxygen adsorbed on-surface at $\frac{1}{4}$ ML coverage.

Figure 2 shows that Au/R-TiO_2 binds oxygen more strongly than Au/R-SiO_2 and stretched Au(111) for all examined oxygen coverages and configurations. The observed behavior is not a consequence of the TiO_2-induced Au lattice stretch but rather it is the result of oxide-specific electronic interactions between the support and Au.

To understand the observed oxide-specific behavior of the Au/oxides we have investigated their electronic structure. When an oxygen vacancy is created on an oxide, two electrons remain in the vacancy. The redistribution of this electron density is oxide specific. Figure 3(a) shows the

local density of states (LDOS) projected onto the bridge Ti and Si atoms of the stoichiometric and vacancy-rich versions of the respective oxides. The Ti LDOS suggests that the electron density, freed upon the formation of the vacancy, shifts to low laying $3d$ bands of the neighboring bridge Ti atoms. These orbitals are unoccupied in the stoichiometric S-TiO_2. Bader charge analysis shows that the bridge Ti atoms gain $\sim 0.4e^-$ each and move apart by additional 1 Å, compared to the Ti-Ti distance in S-TiO_2. Figure 3(a) also shows the localized Wannier orbital corresponding to a $3d$ state that gains the electron density from the vacancy.

On the other hand, the Si-projected LDOS shows that the electron density, freed upon the formation of the oxygen vacancy on SiO_2, is utilized to form a Si-Si bonding state at ~ 0.85 eV below the Fermi level. This electron density is localized along the Si-Si bond, which is formed at the oxygen vacancy. This is corroborated by the Wannier orbital corresponding to this state, shown in Fig. 3(b). The formation of the Si-Si bond is also supported by the fact that the Si-Si distance is shortened from ~ 2.8 Å for S-SiO_2 to ~ 2.6 Å. The oxide-specific electron density redistribution has significant impact on the chemical behavior of Au deposited on the oxide surfaces.

When Au is deposited on R-TiO_2, there is a considerable chemical interaction between the Au and the oxide which

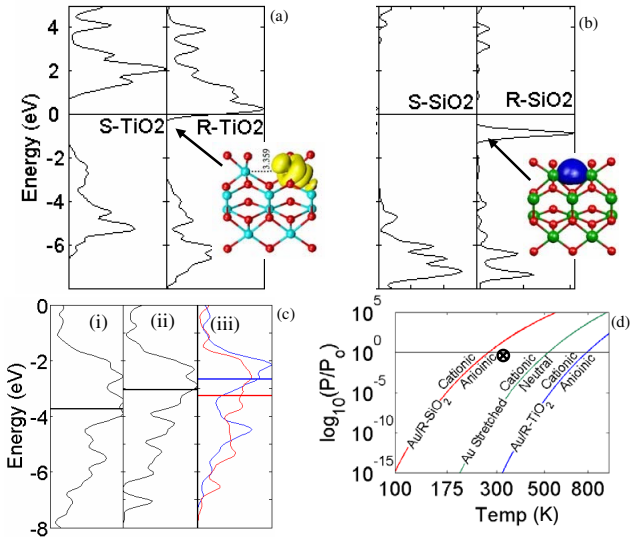

FIG. 3 (color online). (a) Bridge Ti-projected LDOS for S-TiO_2 and R-TiO_2. The inset shows the Wannier orbital corresponding to Ti $3d$ state that gains electron density. (b) Bridge Si-projected LDOS for S-SiO_2 and R-SiO_2. The inset shows the Wannier orbital corresponding to the Si-Si binding state of R-SiO_2. (c) LDOS projected on an Au atom in the top Au layer for: (i) Au(111), (ii) stretched Au(111), (iii) Au/R-TiO_2 (blue line), and Au/R-SiO_2 (red line). Horizontal blue and red lines show the position of the center of the Au LDOS for Au/R-TiO_2 and Au/R-SiO_2, respectively. (d) The lines depict external pressure and temperature at which the average electronic fingerprint of Au changes from anionic to cationic (oxidized). The large dot represents typical CO-oxidation conditions.

results in high Au bilayer binding energy, calculated to be -1.97 eV per vacancy. The electron density, accumulated in the Ti $3d$ states upon the vacancy formation, is redistributed as Au-Ti bonds are formed. This density is not only localized along the Ti-Au bonds but it is distributed among neighboring Au atoms. We calculate that the Bader charge on the Au atom at the oxygen vacancy is $\sim 0.46e^-$, while the Au atoms in the top Au layer gain $\sim 0.1e^-$ per atom. Bader charge analysis suggests the formation of anionic $Au^{\delta-}$, which is in agreement with other theoretical calculations [6,7,18] and with UHV experiments [3]. The driving force for the observed electron density shift is that the Au/R-TiO_2 system can reduce its energy by electron transfer from Ti $3d$ states to energetically lower Au states.

Compared to Au/R-TiO_2, the interaction between Au and R-SiO_2 is weaker as corroborated by the lower Au bilayer binding energy, calculated to be -1.07 eV per vacancy. Bader charge analysis indicates that only $\sim 0.22e^-$ are transferred from R-SiO_2 to the Au atom at the vacancy. The calculated Bader charge transfer is a consequence of the covalent charge localization along the bridge-Si-Au bonds. Unlike in the case of Au/R-TiO_2, the Au atoms in the top layer do not gain electron density.

The proposed oxide-specific interactions between Au and the vacancy-rich oxides are further supported by the LDOS projected on an Au atom in the top Au layer, shown in Fig. 3(c). The Au LDOS associated with Au/R-TiO_2 has shifted upward in energy more than the Au LDOS associated with Au/R-SiO_2 and stretched Au(111). The accentuated shift upward in the Au LDOS for Au/R-TiO_2 is another consequence of the larger electron density transfer from R-TiO_2 than from R-SiO_2.

The extent of the electron density transfer from R-TiO_2 and R-SiO_2 to Au impacts the chemical behavior of Au nanostructures deposited on these oxides. One manifestation of this is that an Au atom cohesive energy for Au/R-TiO_2 is lower than the respective cohesive energies for Au/R-SiO_2 and stretched Au(111). This has a direct impact on the chemical activity since the low Au cohesive energy allows for a less rigid Au nanostructure, which can easily adjust its geometry to adsorbates and relevant transition states and yield reaction pathways with low activation barriers. Also, due to their anionic character, the Au atoms adsorbed on R-TiO_2 interact strongly with electronegative adsorbates such as oxygen. We calculate that the adsorption energy of molecular O_2 adsorbed on Au/R-TiO_2 is by ~ 0.5 and 0.3 eV more exothermic than for O_2 on Au/R-SiO_2 and stretched Au(111), respectively. The main interaction is through electron charge transfer from anionic $Au^{\delta-}$ to O_2 antibonding $2\pi^*$ orbital. This charge transfer weakens significantly the O_2 bond. Similarly, atomic oxygen binds more strongly to Au/R-TiO_2 than to stretched Au(111) or to Au/R-SiO_2 as illustrated in Fig. 2. These results suggest that O_2 activation is energetically more favorable over Au nanostructures on R-TiO_2 than over Au/R-SiO_2 and stretched Au. Whether O_2 activation is unimolecular or it requires coadsorbates is an

interesting problem in its right. Since this is not the focus of this Letter we will elaborate on the issue in future communications.

We calculate that highly anionic Au, formed when Au is deposited on R-TiO_2, binds oxygen stronger than Au/R-SiO_2. This observation might explain the apparent paradox discussed above, where UHV experiments and DFT calculations showed that Au adsorbed on oxides is negatively charged (anionic), while steady-state studies suggested that the activity of Au/oxide catalysts is directly proportional to the concentration of cationic Au atoms. Simply stated, anionic Au is needed to adsorb and activate O_2. However, as Au-oxygen bonds are formed, the electronic fingerprint of Au is reversed from anionic to cationic due to the high electronegativity of oxygen. This behavior is illustrated in Fig. 3(d), which shows the Au electronic fingerprint as a function of the support and external conditions [19]. Under low oxygen chemical potential, corresponding to low pressure (UHV conditions) and high temperature, Au is anionic when adsorbed on both oxides. As oxygen chemical potential is increased the interactions between oxygen and Au/oxide are turned on, eventually yielding oxidized (cationic) $Au^{\delta+}$. The transition from anionic to cationic Au takes place at a lower oxygen chemical potential for Au/R-TiO_2 than for Au/R-SiO_2. Our *ab initio* thermodynamic calculations suggest that under catalytically relevant conditions there exists a thermodynamic driving force to oxidize the regions of Au nanostructure that are close to the R-TiO_2 vacancies, while for Au/R-SiO_2 these regions will not oxidize at these conditions [19]. We note that cationic Au, formed in the process of the Au-oxygen bond formation, interacts with CO and propylene favorably, therefore providing an ideal environment for the low-temperature oxidation reactions [20].

The above described studies suggest a simple mechanism that might be able to account for the observed oxide-specific catalytic activity of supported Au nanostructures. Reducible oxides such as TiO_2, which are characterized by a small band gap, accommodate the electron density, released upon oxygen-vacancy formation, by the charge transfer to low laying d states. The electronic charge accommodated in the Ti 3d states, which cut through the R-TiO_2 Fermi level, is readily transferred to Au. On the other hand, irreducible oxides such as SiO_2, which are characterized by a larger band gap, undergo geometric restructuring, and Si-Si binding states are formed at the vacancy. The charge transfer from R-SiO_2 to Au is limited due to the fact that the Si-Si binding states are stabilized below the Fermi level. Since more charge is transferred from reducible oxides to Au, the Au adsorbed on these oxides interacts more strongly with oxygen providing an ideal environment for O_2 activation and for the oxidation reactions. The capacity of Au atoms adsorbed on reducible oxides, such as TiO_2, to be readily oxidized and reduced at mild conditions might explain the unique low-temperature oxidation activity of Au nanostructures adsorbed on reducible oxides.

*Corresponding author.
Electronic address: linic@umich.edu

[1] M. Haruta, Catal. Today **36**, 153 (1997).
[2] M. Valden, X. Lai, and D. W. Goodman, Science **281**, 1647 (1998).
[3] T. Minato, T. Susaki, S. Shiraki, H. S. Kato, M. Kawai, and K. Aika, Surf. Sci. **566–568**, 1012 (2004).
[4] J. Guzman and B. C. Gates, J. Am. Chem. Soc. **126**, 2672 (2004).
[5] L. Fu, N. Q. Wu, J. H. Yang, F. Qu, D. L. Johnson, M. C. Kung, H. H. Kung, and V. P. Dravid, J. Phys. Chem. B **109**, 3704 (2005).
[6] L. M. Molina and B. Hammer, Phys. Rev. B **69**, 155424 (2004).
[7] Z. P. Liu, S. J. Jenkins, and D. A. King, Phys. Rev. Lett. **93**, 156102 (2004).
[8] B. Yoon, H. Hakkinen, U. Landman, A. S. Worz, J. Antonietti, S. Abbet, K. Judai, and U. Heiz, Science **307**, 403 (2005).
[9] S. D. Lin, M. Bollinger, and M. A. Vannice, Catal. Lett. **17**, 245 (1993).
[10] S. Arrii *et al.*, J. Am. Chem. Soc. **126**, 1199 (2004).
[11] E. Wahlstrom, N. Lopez, R. Schaub, P. Thostrup, A. Ronnau, C. Africh, E. Laegsgaard, J. K. Norskov, and F. Besenbacher, Phys. Rev. Lett. **90**, 026101 (2003).
[12] M. S. Chen and D. W. Goodman, Science **306**, 252 (2004).
[13] S. Giorgio, C. R. Henry, B. Pauwels, and G. Van Tendeloo, Mater. Sci. Eng. A **297**, 197 (2001).
[14] We utilize periodic pseudopotential plane wave DFT calculations with GGA-PW91 functional (http://www.camp.dtu.dk). The calculations were converged with respect to k-point sampling, number of oxide layers, plane wave cutoff, and the force convergence threshold of 0.05 eV/Å. The top 2 Au layers are relaxed in the z direction while oxygen adsorbates were relaxed in all three directions. We have performed a number of studies, for different oxygen-vacancy concentrations, where all Au and O atoms were allowed to fully relax in all directions. While, depending on the oxygen-vacancy concentration, there might be surface restructuring and shifts in oxygen adsorption energy, the results of the fully relaxed calculations are in qualitative agreement with the results reported in Fig. 2.
[15] W. X. Li, C. Stampfl, and M. Scheffler, Phys. Rev. Lett. **90**, 256102 (2003).
[16] K. Reuter and M. Scheffler, Phys. Rev. B **65**, 035406 (2002).
[17] D. R. Stull and H. Prophet, *JANAF Thermochemical Tables* (U.S. NBS, Washington, DC, 1971), 2nd ed..
[18] D. Pillay and G. S. Hwang, Phys. Rev. B **72**, 205422 (2005).
[19] Anionic/cationic transition lines will be affected by the ability of an oxidizing agent such as CO to reduce the substrate, and the ability of the substrate to activate O_2.
[20] Z. P. Liu, S. J. Jenkins, and D. A. King, Phys. Rev. Lett. **94**, 196102 (2005).